

The Effect of Torsion Stress on the Circumferential Permeability of CoFeBSi Amorphous Wires

I. Betancourt and R. Valenzuela

Abstract—In this paper, a domain model and the complex inductance formalism are employed to study the effect of torsion stress on the low-frequency magnetoimpedance (MI) response of CoFeBSi amorphous wires (125 μm in diameter). In particular, the torsional dependence of the calculated circumferential permeability μ_ϕ is found to be very sensitive to the wire's scalar permeability μ_{dc} which, in turn, depends inversely on the wire's induced anisotropy K_i . Calculated μ_ϕ exhibited a marked increase for increased μ_{dc} and a decrease for reduced μ_{dc} . Experimental spectroscopic plots of μ_ϕ under various torsion stresses (counter- and clockwise-oriented) which resulted in various helically induced anisotropies K_h are consistent with an enhancement/counterbalancing effect of K_i through the addition/subtraction of K_h to K_i .

Index Terms—Complex inductance, induced anisotropy, magnetoimpedance, torsion stress.

I. INTRODUCTION

MAGNETOIMPEDANCE (MI) refers to the variations in the impedance response of soft magnetic materials (subjected to a high-frequency current i_{ac} of small amplitude) when a dc magnetic field is applied. Considerable interest has been raised in MI materials due to their sensing technology applications [1]. This phenomenon is large in vanishing negative magnetostriction amorphous wires because of their particular domain structure: an axially oriented core, surrounded by circumferential domains (bamboo-like structure). This domain configuration is afforded by the wire's induced anisotropy K_i , which arises from the coupling between magnetostriction and internal stresses during the fabrication process [2], [3]. Due to this magnetoelastic coupling, MI is strongly sensitive to both tensile stress [4] and torsional strain [5]. The frequently used magnetoimpedance ratio $\Delta Z/Z_0$ for monitoring MI response employed in most reports does not allow a simple physical interpretation, since at a low-frequency regime, no $\Delta Z/Z_0$ variation is observed [6]. In contrast, the complex inductance formalism [7] affords a more clear physical insight into the magnetization process, since magnetization mechanisms at low frequencies (e.g., reversible domain wall bulging and unpinning displacement of domain walls) can be resolved through the calculation of the complex permeability $\mu = \mu_{real} - j\mu_{imag}$ from

the complex impedance, $Z = Z_{real} + jZ_{imag}$ via the following transformation [8]:

$$\mu = G \left(\frac{-jZ}{\omega} \right) \quad (1)$$

where ω is the angular frequency of i_{ac} (and, hence, of h_{ac}) and G is a geometrical factor $G \sim 10^8(\text{henry})^{-1}$ [8]. In (1), μ_{real} corresponds to the wire circumferential permeability μ_ϕ (since the applied field h_{ac} has also a circumferential character), whereas μ_{imag} is associated with dissipative processes. In addition, it is also possible to calculate circumferential magnetization curves $M_\phi(h_{ac})$ by means of [6]

$$\mu_o M_\phi = h_{ac} \left(G \left(\frac{Z_{imag}}{\omega} \right) - \mu_o \right). \quad (2)$$

On the other hand, a domain model reported recently for the MI of ferromagnetic wires [9], [10] establishes exact analytical expressions for the real and imaginary components of the complex impedance Z . An important parameter for calculation is the scalar dc permeability μ_{dc} , which depends inversely on the restoring pinning force coefficient per unit wall area α : $\mu_{dc} = C/\alpha$ ($C = \text{constant}$). This restoring coefficient is proportional to the domain wall energy γ , which, in turn, depends on K_i [11] and, thus, $\mu_{dc} = C/K_i$. By using the Z_{real} , Z_{imag} exact expressions and (1), we study the effect of μ_{dc} variations on μ_ϕ and compare with experimental μ_ϕ subjected to various torsional stresses which affect directly K_i .

II. EXPERIMENTAL TECHNIQUES

As-cast amorphous $(\text{Co}_{94}\text{Fe}_6)_{72.5}\text{B}_{15}\text{Si}_{12.5}$ wires, 10-cm length and 125- μm diameter, prepared by the in-rotating-water spinning method, were used for spectroscopic measurements. Samples were mounted in a special sample holder with firm electrical contacts that enabled the application of controlled torsional stresses both in the clockwise (+) and in the counterclockwise (−) directions. The measuring system includes an HP 4192 A impedance analyzer controlled by a PC. Our measuring software allows the determination of the complex impedance for 94 discrete frequencies within the range 5 Hz–13 MHz.

III. RESULTS AND DISCUSSION

Calculated μ_{real} and μ_{imag} plots are shown in Fig. 1. The variations for an initial value of $\mu_{dc} = 0.004241 \text{ H/m}$ (determined for a torsion-free 10-cm-length CoFeBSi amorphous wire) are taken as $2 \mu_{dc}$ and $0.5 \mu_{dc}$. The low-frequency initial constant

Manuscript received January 3, 2003. This work was supported in part by DGAPA-UNAM, Mexico, under Grant IN111200.

The authors are with the Instituto de Investigaciones en Materiales, National University of Mexico, Coyoacan, México D.F. 04510, Mexico (e-mail: israelb@correo.unam.mx).

Digital Object Identifier 10.1109/TMAG.2003.816016

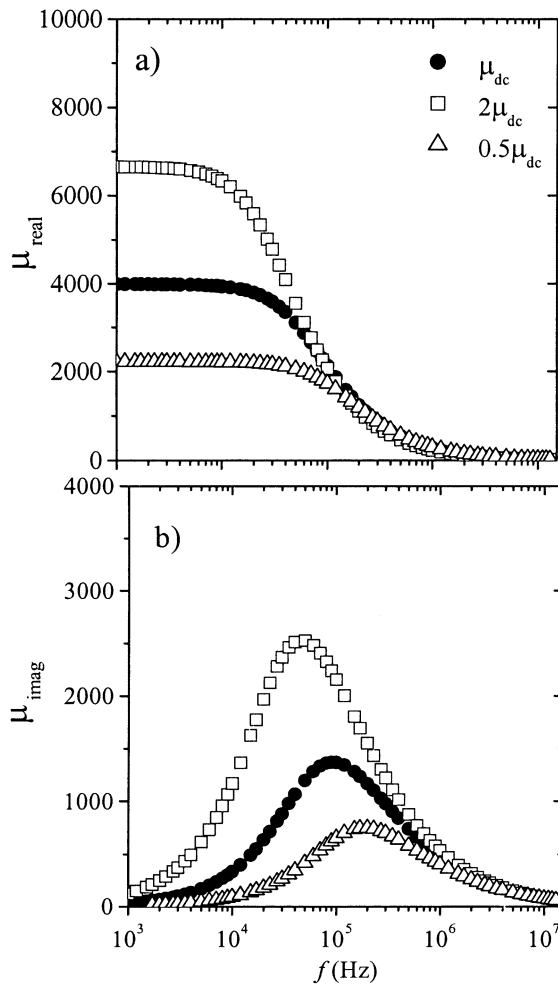


Fig. 1. Calculated spectroscopic plots of a) μ_{real} and b) μ_{imag} for various μ_{dc} values.

μ_{real} dependence (which corresponds to μ_{ϕ} [7]) increases with increased μ_{dc} and decreases with diminished μ_{dc} . On the other hand, the maximum in μ_{imag} (associated with the relaxation frequency f_x for which the domain bulging mechanism is no longer active and for which μ_{real} manifest a relaxation dispersion when $f > f_x$ [7]) shifts to lower frequencies with enhanced μ_{dc} and moves forward with smaller μ_{dc} values.

As mentioned above, μ_{dc} is inversely proportional to K_i . Therefore, it is reasonable to ascribe μ_{dc} variations to a varying K_i , which can be affected directly by helically induced anisotropies K_h produced by torsion stresses. This assumption is in agreement with Fig. 2 for which experimental spectroscopic μ_{real} and μ_{imag} plots corresponding to (+) and (-) torsion angles are shown. The $+90^\circ$ curve exhibits an enhancement of μ_{real} together with a decreased f_x in μ_{imag} , while for the -90° curve, a reduced μ_{real} accompanies higher f_x values in μ_{imag} . This enhancement/detrimental behavior on μ_{real} is consistent with a counterbalancing effect of K_h on K_i for (+) torsion angles, whereas (-) torsion angles produce K_h , which reinforce K_i . Notice the remarkable agreement between calculated and experimental plots (Figs. 1 and 2) on both real and imaginary components. In addition, calculated μ_{real} plots merge into a single curve for $f > f_x$ as their measured counterpart. On the other hand, calculated μ_{imag} at

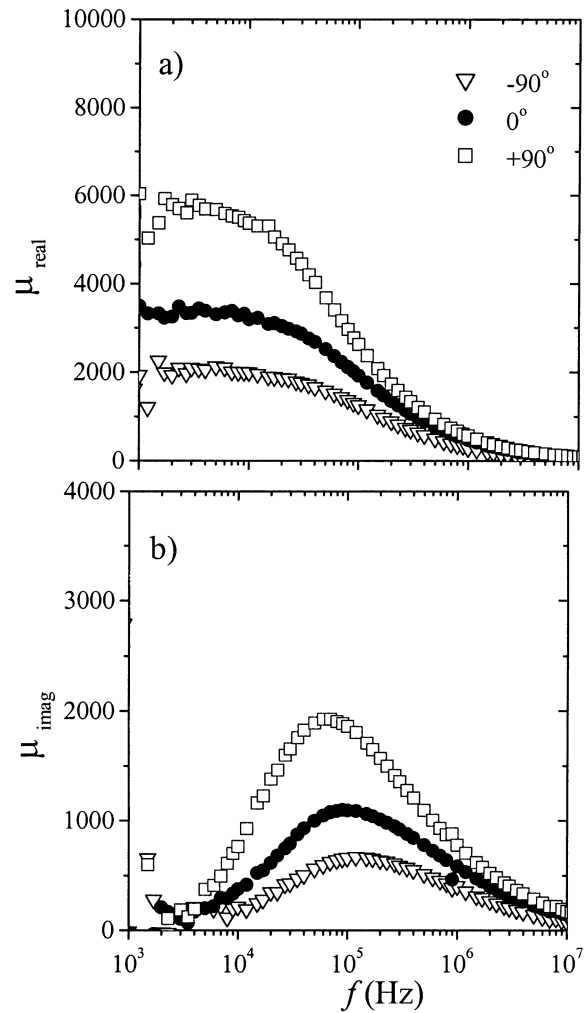


Fig. 2. Experimental spectroscopic plots of a) μ_{real} and b) μ_{imag} for various torsion angles.

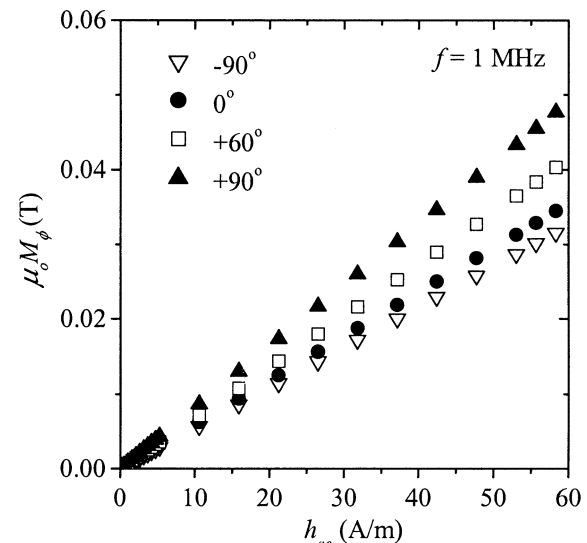


Fig. 3. Measurements of circumferential magnetization as a function of h_{ac} field at $f = 1$ MHz, for various torsion angles.

original μ_{dc} exhibits a maximum at ~ 100 kHz, which agrees very well with the experimental one. The effect of the torsion stress on wire's anisotropy is also manifested in Fig. 3, where

circumferential magnetization, M_ϕ , is plotted as a function of the applied ac field h_{ac} at a frequency of 1 MHz, well above f_x . At this frequency, the domain wall displacement mechanism is no longer active and spin rotation remains as the only magnetization process, leading to a linear dependence of $M_\phi(h_{ac})$. As the torsion stress compensates K_i at (+) angles, the slope of the plot increases, which affords higher M_ϕ ; conversely, for (-) torsion angles, the decreasing slope reflects an increment in K_i .

IV. CONCLUSION

By using a model for MI in ferromagnetic wires, we have shown that torsion stresses add (or subtract) to the helically induced anisotropy in a CoFeSiB wire, leading to a decrease (or an increase, depending on the torsion direction) on its scalar dc permeability and, thus, to an enhanced/reduced circumferential permeability.

REFERENCES

- [1] M. Vazquez, "Giant magnetoimpedance in soft magnetic wires," *J. Magn. Magn. Mater.*, vol. 226–230, pp. 693–699, 2001.
- [2] M. Vazquez and A. Hernando, "A soft magnetic wire for sensor applications," *J. Phys. D: Appl. Phys.*, vol. 29, pp. 939–949, 1996.
- [3] P. T. Squire, D. Atkinson, M. R. J. Gibbs, and S. Atalay, "Amorphous wires and their applications," *J. Magn. Magn. Mater.*, vol. 132, pp. 10–21, 1994.
- [4] M. T. González, K. L. García, and R. Valenzuela, "Circumferential magnetization curves of Co-rich amorphous wires under tensile stress," *J. Appl. Phys.*, vol. 85, pp. 319–324, 1999.
- [5] J. M. Blanco, A. Zhukov, and J. Gonzalez, "Effect of tensile and torsion on GMI in amorphous wire," *J. Magn. Magn. Mater.*, vol. 196–197, pp. 377–379, 1999.
- [6] I. Betancourt and R. Valenzuela, "Influence of the torsion stress on the circumferential magnetization curves of CoFeBSi amorphous wires," *Appl. Phys. Lett.*, vol. 81, pp. 94–96, 2002.
- [7] R. Valenzuela, "Low-frequency magnetoimpedance: Domain wall magnetization processes," *Physica B*, vol. 299, pp. 280–285, 2001.
- [8] M. L. Sanchez, R. Valenzuela, M. Vazquez, and A. Hernando, "Circumferential permeability in nonmagnetostrictive amorphous wires," *J. Mater. Res.*, vol. 11, pp. 2486–2489, 1996.
- [9] D. X. Chen, J. L. Muñoz, A. Hernando, and M. Vazquez, "Magnetoimpedance of metallic ferromagnetic wires," *Phys. Rev. B*, vol. 57, pp. 10 699–10 704, 1998.
- [10] D. X. Chen and J. L. Muñoz, "AC impedance and circular permeability of slab and cylinder," *IEEE Trans. Magn.*, vol. 35, pp. 1906–1923, 1999.
- [11] K. L. García and R. Valenzuela, "The effects of the axial DC field on magnetoimpedance: Circumferential domain wall damping," *IEEE Trans. Magn.*, vol. 34, pp. 1162–1164, July 1998.